Scaling Electrochemical Battery Models for Time-Accelerated and Size-Scaled Experiments on Test-Benches

Javier Cabello, Xavier Roboam, Sergio J. Junco, Eric Bru, Fabien Lacressonnière

Scaling Electrochemical Battery Models for Time-Accelerated and Size-Scaled Experiments on Test-Benches

J. M. Cabello, X. Roboam, S. Junco, E. Bru and F. Lacressonniere

***Abstract*—This article presents a dimensional-analysis supported scaling procedure applied to a mathematical model of electrochemical batteries. The main objective of this research is to allow for laboratory size-scaled and time-compressed experimental analysis of processes involving large physical magnitudes and evolving over long time spans. These situations are of interest when considering the sizing of battery packs and other components of energy systems, particularly smart grids, and further systems where battery storage is relevant, like hybrid vehicles and other standalone systems, as well as deciding management strategies on them. Voltage-, current- and time-scaled models preserving the dynamic evolution of a group of relevant physical magnitudes are presented. These models have been validated through simulation and physical experiments on a test-bench designed and constructed on purpose. The physical implementation of the scaled models is not possible in the cases where some of the scaled model parameters cannot be met using real batteries. But, as the mathematical construction of the scaled models is always possible, this problem can be circumvented with a Hardware-in-the-loop approach: the scaled battery is numerically emulated on a programmable and controllable power source/sink system, which is run in real-time embedded in the test-bench representing the whole system under study.**

***Index Terms*—Battery Models, Battery System Testing, Similarity, Scaled systems, Time Acceleration.**

I. Introduction

NONDIMENSIONALIZATION of models of physical systems is a successful method used in science and engineering. Different application domains have developed different approaches for nondimensionalizing the systems object of their studies. Well known are, for instance, the normalization techniques yielding so-called "per unit" systems, which refer the values of the physical magnitudes to certain values of reference or base variables. This is the case in electrical engineering, where given values of power, voltage and angular frequency are used (in the study of electrical power systems, for instance, see [1]), or values of voltage, electrical current and rotational speed (when studying the dynamics of rotary electrical machines [2]). Widely spread in science and engineering are the methods derived from dimensional analysis [3], [4], a technique based on the fact that the laws of physics must be independent of the units employed to assign values to the physical magnitudes. These methods, with –probably– fluid-dynamics being their most prominent realm of application, allow for reducing the number of physical parameters of a problem to a lesser number of dimensionless combinations of them (dimensionless groups), to establish functional relationships between certain properties of nondimensionalized variables and the dimensionless groups, to gain insight into general properties of similar systems on the sole dependency of these groups, and to conduct studies on scaled systems with results being transferable to the system of interest thanks to the property of similarity [5].

Nondimensionalization can be advantageously used on both, mathematical and physical models, in the former case, for instance, to properly determine negligible terms in mathematical expressions or to reduce the amount of computations when analyzing system behavior in parameter space and, in the latter case, to conduct experiments in physical scale models that replicate the behavior of the original systems. The coupling via actuators and smart sensors of physical systems with computing devices running algorithms in real time integrates these two originally separated application domains. This situation arises in the standard computer-controlled systems and, lately at a dramatically increasing pace, in Hardware-In-the-Loop (HIL) systems [6]-[9], where for instance, prototype controllers are physically tested on experimental set-ups consisting either of the real plant to be controlled or of a scale model as its physical emulator, such as in reported in [10]. Scaling is necessary here as a means to adapt the amplitude of the magnitudes being handled at the interface between the physical system and the processors involved in the actuators and sensors. Also because of the numerical treatment of the data in these processors some sort of scaling is almost always mandatory.

The motivation of the present study is to provide experimental analysis and validation tools for the design of engineering systems including electrochemical batteries as

This work was supported in part by CONICET (the Argentine National Council for Scientific and Technological Research), SeCyT-UNR (the Secretary for Science and Technology of the National University of Rosario), ANPCyT (PICT 2012 Nr. 2471) and the scholarship program Saint-Exupery.

J.M. Cabello and S. Junco are with the Laboratorio de Automatización y Control, Facultad de Ciencias Exactas, Ingeniería y Agrimensura (FCEIA), Universidad Nacional de Rosario (UNR), Argentina (e-mail:{jcabello;sjunco}@fceia.unr.edu).

E. Bru, X. Roboam and F. Lacressonniere are with the Université de Toulouse, LAPLACE, UMR 5213 CNRS-INPT-UPS, Toulouse, France (e-mail:{eric.bru;xavier.roboam;fabien.lacressonniere}@laplace.univ-tlse.fr).

storage components. These are model-related tools that should allow to develop test benches scaled in power, energy and/or time acting as physical emulators of the systems under study. The article focuses particularly on the scaling through dimensional analysis of a specific model of electrochemical Li-Ion batteries, an ubiquitous storage component in smart grids with renewable sources, hybrid vehicles, airplanes, among others. As detailed later, the battery port-variables voltage and current, as well as time, are the scaled variables.

A dimensional-analysis based scaling of a basic electrochemical battery model is presented in [11] in the context of design and evaluation of a Hybrid Electric Vehicle (HEV). In [6] a scaling procedure of a more complex model, where the dynamic behavior and nonlinearities of the battery are taken into account, is implemented in a HIL system and experimentally validated, but this procedure is done ad-hoc. In the particular context of vehicle powertrain simulation, a dimensional-analysis based method is developed in [10] to derive input/output scaling factors which, among other studies, is applied to a complex dynamic battery model simulation, experimentally complemented on actual hardware.

Proceeding in a similar manner as in [10], this article formalizes the procedure of size scaling developed in [6] (though on a different, refined model) using dimensionless variables, as defined by the Pi-theorem [12]. This formalization assures the dimensional similarity of original and scaled models, which, among other advantages, allows for the easy extension of the procedure to time scaling. Results of both, numerical and physical experimental tests designed to validate these scaling procedures are reported. It is shown that the construction of a perfect physical emulator (physical scale model) of an electrochemical battery is not always possible due to the existence of physical constraints among the parameters of the model, that cannot be overcome by the degrees of freedom available to configure the physical emulator (there is no battery interconnection capable of reproducing some of the scaled parameters). Nevertheless, numerical emulation of the scaled model is always possible, what opens up the possibility of running the scaled model on-line in real-time on a computer associated to a programmable power source/sink, and thus to embed it on a HIL-system, see Fig. 1.

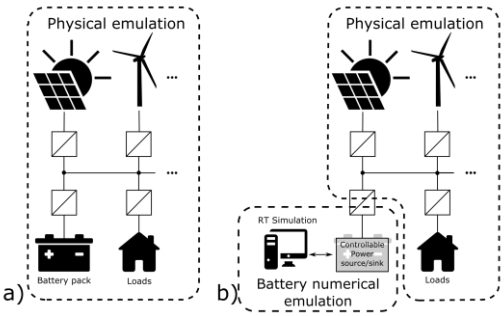

Fig. 1. Electric power system emulation schemes for: a) Complete physical emulation. b) Physical emulation with numerical emulation of the battery.

The remainder of this work is organized as follows: In Section 2 the battery model is specified and the dimensional-analysis supported scaling procedure is developed. In Section 3 the procedure is applied to obtain mathematical scale models which are validated via numerical simulation. Section 4 deals with the implementation of a physical scale model; first, the test bench setup is presented, then the scale procedure is applied to define the physical implementation and, finally, validation experiments are reported. Section 5 summarizes the main conclusions.

II. Scaling of Electrochemical Battery

The aim of this research is reducing both component size and testing time on experimental studies related to smart grids problems (system sizing; grid architecture, topology and energy management definition; testing controller performance, etc.) Nevertheless, the results are applicable as well to many types of systems processing electric energy from embedded storages. Other phenomena not considered in the model used in this research can be as well handled with this time accelerated approach, for instance, changes in parameter values (capacity, internal resistance, etc.) due to the degradation of the battery (ageing/cycling).

Energy storage systems are essential in providing energy management alternatives in smart electrical grids. They allow for increased integration to the grid of renewable energy sources as well as for improved reliability and stability of various systems [13]. Electrochemical batteries of diverse technologies such as Lead-Acid (Ld), Nickel-Cadmium (Ni-Cd), Nickel-Metal Hydride (Ni-MH) and Lithium-Ion (Li-Ion) constitute the most widely used class of available storage systems [14]. As they are not only key but also rather expensive components of smart grids, engineering decisions concerning the integration of batteries into smart grids need the support of reliable experimental results, which can be best provided by emulation of these smart grids on physical scale models.

A. Battery Model

There are several battery models of diverse complexity and accuracy [15]. Here, the extension presented in [17] of the commonly used analytic semi-empiric Tremblay-Dessaint battery model [16] is used, which allows for an accurate reproduction of the battery output voltage without increasing the model complexity. It consists of the two port-variables Voltage and Current (essential magnitudes related to battery performance and control), the two state variables State of Charge (related to the battery usage and stored energy) and Filtered Current (captures a delay in voltage evolution), as well as 8 parameters. It can be summarized as follows:

$$\begin{aligned} \frac{d}{dt}\,SoC &= -\frac{1}{Q}\,i \\ \frac{d}{dt}\,i^* &= -\frac{1}{Tf}i^* + \frac{1}{Tf}i \\ v &= E_0 + Ae^{-BQ(1-SoC)} - K_1 Q\left(\frac{1}{SoC}-1\right) - Ri \\ &\quad - K_2\,i^*\left(\frac{is_{dch}}{SoC} + \frac{is_{ch}}{1.1-SoC}\right) \end{aligned} \tag{1}$$

where the variables are the battery discharge current i (A), the State of Charge SoC (-), the filtered discharge current i^* (A) and

the battery voltage v (*V*). The parameters are the battery capacity Q (*Ah*), the current-filter time constant T_f (*s*), the battery constant voltage E_0 (*V*), the exponential-zone amplitude A (*V*), the exponential-zone inverse capacity B (Ah^{-1}), the polarization constant K_1 (*V/Ah*), the internal resistance R (Ω) and the polarization resistance K_2 (Ω). The logic variables is_{dch}, being 1 when the battery is discharging and 0 otherwise, and is_{ch}, being 1 when the battery is charging and 0 otherwise, have been introduced to condense notation.

B. Dimensional analysis

The scaling procedure presented next is justified by a *dimensional analysis* of the previous battery model, which provides a number of dimensionless variables or groups, or π-groups. As known from similarity theory, two systems of the same nature have the very same behavior (under the same experimental conditions) provided that these π-groups have the same values for the two systems, which are then said to be *dimensionally similar*. This property allows studying the behavior of the system of interest experimenting on another one, similar to the former, on a more convenient physical scale.

The nondimensionalization procedure, as described in [4], starts by identifying the set of relevant quantities, i.e., the physical quantities (constant, variables and parameters) used to describe the phenomenon under study. Analyzing (1) yields the following 13 relevant quantities (recall that the logic variables is_{dch} and is_{ch} are not considered because they do not represent physicals variables or parameters):

$$\{E_0, B, Q, A, K_1, T_f, R, K_2, t, v, i, i^*, SoC\}$$

The *dimensional formula* of each quantity based on fundamental units (MKSA units) is:

$$\begin{array}{l} [E_0] = m^2 kg\ s^{-3}A^{-1}; [B] = A^{-1}s^{-1}; \quad [Q] = A\ s \\ [A] = m^2 kg\ s^{-3}A^{-1}; [R] = m^2 kg\ s^{-3}A^{-2}; \ [T_f] = s \\ [K_1] = m^2 kg\ s^{-4}A^{-2}; [K_2] = m^2 kg\ s^{-3}A^{-2}; [t] = s \\ [v] = m^2 kg\ s^{-3}A^{-1}; \ [i] = A; \ [i^*] = A; \ [SoC] = 0 \end{array} \quad (2)$$

The number of fundamental dimensions are 4, but as m^2 and kg are always together, the combined unit $m^2 kg$ is used as a base unit reducing the number of dimensions to **3**. Hence, according to the π-theorem [3], [4], [12], the number of non-dimensional groups (π- groups) is 10 (**13 – 3** = **10**).

TABLE I
DIMENSIONAL SET MATRIX

A_{dim}	A	B	K_1	R	K_2	i	i^*	v	t	SoC	E_0	Q	T_f	B_{dim}
A	-1	-1	-2	-2	-2	1	1	-1	0	0	-1	1	0	
s	-3	-1	-4	-3	-3	0	0	-3	1	0	-3	1	1	
m^2kg	1	0	1	1	1	0	0	1	0	0	1	0	0	
π_1	1	0	0	0	0	0	0	0	0	0	-1	0	0	
π_2	0	1	0	0	0	0	0	0	0	0	0	1	0	
π_3	0	0	1	0	0	0	0	0	0	0	-1	1	0	
π_4	0	0	0	1	0	0	0	0	0	0	-1	1	-1	
π_5	0	0	0	0	1	0	0	0	0	0	-1	1	-1	
π_6	0	0	0	0	0	1	0	0	0	0	0	-1	1	
π_7	0	0	0	0	0	0	1	0	0	0	0	-1	1	
π_8	0	0	0	0	0	0	0	1	0	0	-1	0	0	
π_9	0	0	0	0	0	0	0	0	1	0	0	0	-1	
π_{10}	0	0	0	0	0	0	0	0	0	1	0	0	0	
I_{10x10}														C_{rp}

Selecting E_0, Q and T_f as repeating parameters the Dimensional Set Matrix of Table I is created, where the entries of matrices $\boldsymbol{B_{dim}}$ and $\boldsymbol{A_{dim}}$ are the exponents of each dimension in the dimensional formulae given in (2). The matrices I_{10x10} and $\boldsymbol{C_{rp}}$ allow to set the π-groups; $\boldsymbol{C_{rp}}$ is calculated as $\boldsymbol{C_{rp}} = -\left(\boldsymbol{A_{dim}^{-1}B_{dim}}\right)^{\boldsymbol{T}}$. Table I yields the following π-groups:

$$\pi_1 = \frac{A}{E_0} \quad \pi_2 = BQ \quad \pi_3 = \frac{K_1 Q}{E_0} \quad \pi_4 = \frac{RQ}{T_f E_0}$$
$$\pi_5 = \frac{K_2 Q}{T_f E_0} \quad \pi_6 = \frac{i\, T_f}{Q} \quad \pi_7 = \frac{i^*\, T_f}{Q} \quad \pi_8 = \frac{v}{E_0} \quad (3)$$
$$\pi_9 = \frac{t}{T_f} \quad \pi_{10} = SoC$$

Two different π-groups can be distinguished: The π-parameters (π_1,…, π_5) and the π-variables (π_6,…, π_{10}).

Substituting the previous π-groups (3) in (1) the following dimensionless system model is obtained:

$$\frac{d}{d\pi_9}\pi_{10} = -\pi_6$$
$$\frac{d}{d\pi_9}\pi_7 = -\pi_7 + \pi_6 \quad (4)$$
$$\pi_{8(\pi_{10},\pi_7,\pi_6)} = \pi_1 + \pi_2 e^{-\pi_2(1-\pi_{10})} - \pi_3\left(\frac{1}{\pi_{10}} - 1\right) - \pi_4\pi_6 - \pi_5\pi_7\left(\frac{is_{dch}}{\pi_{10}} + \frac{is_{ch}}{1.1 - \pi_{10}}\right)$$

C. Scaling method

The objective of the scaling method is to obtain a new set of parameters for the battery model in order to produce scaled evolutions of the variables indicated below, while the other system variables remain unchanged:

Voltage scaling: Voltage will be affected by a factor of k_v.
Current scaling: Current will be affected by a factor of k_i.
Time scaling: The four system variables will conserve their form but evolving k_t-times faster.

These objectives can be summarized as

$$\begin{array}{c} v_{scaled}(t) \triangleq k_v\, v_{original}(k_t t) \\ i_{scaled}(t) \triangleq k_i\, i_{original}(k_t t) \\ i^*_{scaled}(t) \triangleq k_i\, i^*_{original}(k_t t) \\ SoC_{scaled}(t) \triangleq SoC_{original}(k_t t) \end{array} \quad (5)$$

where the symbol ≙ represents the expected identity to be achieved by parameter adaptation and *t* is the scaled model time. If this adaptation is done correctly both systems will be dimensionally similar, i.e., the π-groups (3) in the original model and the scaled model will be the same. The following equations exemplify the procedure of parameter adaptation.

$$\pi_{8,ori} = \frac{v_{ori}}{E_{0,ori}} \triangleq \pi_{8,sca} = \frac{k_v v_{ori}}{E_{0,sca}} \Rightarrow E_{0,sca} = k_v E_{0,ori}$$
$$\pi_{9,ori} = \frac{k_t t}{T_{f,oril}} \triangleq \pi_{9,sca} = \frac{t}{T_{f,sca}} \Rightarrow T_{f,sca} = T_{f,ori}/k_t$$
$$\vdots$$

Proceeding in the same way for the rest of the π-groups yields the re-parameterization formulae presented in Table II.

TABLE II

PARAMETER CALCULATION OF SCALED MODEL TO ACHIEVE *DIMENSIONAL SIMILARITY*

Parameter	Original model	Voltage-, Current- and Time-scaled model
Q	Q_{ori}	$Q_{ori}\,k_i/k_t$
E_0	$E_{0,ori}$	$E_{0,ori}k_v$
K_1	$K_{1,ori}$	$K_{1,ori}k_v\,k_t/k_i$
A	A_{ori}	$A_{ori}k_v$
B	B_{ori}	$B_{ori}\,k_t/k_i$
R	R_{ori}	$R_{ori}\,k_v/k_i$
K_2	$K_{2,ori}$	$K_{2,ori}\,k_v/k_i$
Tf	Tf_{ori}	Tf_{ori}/k_t

III. MATHEMATICAL SCALE MODELS

In the previous section parameter values of the scaled model were calculated in order to achieve *dimensional similarity* with the original model. The scaled system can be either numerically constructed (aiming at numerical simulation) or physically implemented. Clearly, any parameter value can be specified in a numerical model -hereafter called *mathematical scale model*-, so this numerical implementation is always possible. But when it comes to the physical implementation, or construction of the *physical scale model*, the situation can arise where a parameter value is not attainable because of technological restrictions. This situation happens in the time-scaling case of the battery model, as will be seen more precisely later on this article. The validation of the re-parameterization or scaling procedure is performed next via simulation of the mathematical scale model.

A. *Validation of the mathematical scale model*

The original set of model parameters, given in Table III, corresponds to the parameterization of the lithium-ion cell, VL45E [18]. Three scale models were obtained applying voltage ($k_v = 13$), current ($k_i = 17$) and time ($k_t = 100$) scaling procedures, respectively. Four simulation tests for validation are presented: first, the simulation of the original model with the original set of parameters, and then the simulations for each of the three scale models (voltage-, current-, and time-scaling). The current profile chosen for validation is a realistic two-day current demand profile of an isolated micro smart grid where the battery array is the storage associated to a photovoltaic source. The evolution of all the variables of interest behave as expected, i.e., they are identical, as shown by Fig. 2 (the simulation outputs have been back-scaled using the corresponding factor in each case).

TABLE III
PARAMETER SET OF ORIGINAL MATHEMATICAL MODEL FOR VALIDATION

Parameter	Q (Ah)	E_0 (V)	K_1 (mV/Ah)	A (mV)	B (Ah^{-1})	R $(m\Omega)$	K_2 $(m\Omega)$	Tf (s)
X_ori	45	3.42	0.24	630.8	0.041	3.53	0.24	30

IV. PHYSICAL SCALE MODELS

In order to test and analyse the physical implementation of the scaled models, the link between the battery cell model and the battery system model should be taken into account.

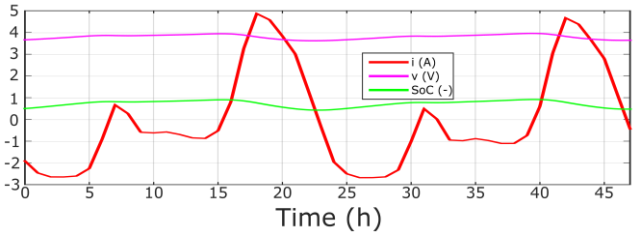

Fig. 2a. Voltage, current and *SoC* evolutions of the original mathematical model under chosen input-current profile.

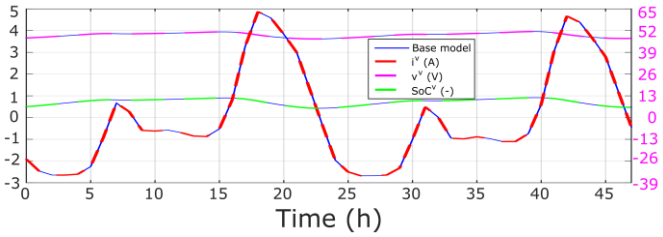

Fig. 2b. Voltage (magenta axis scale), current and SoC evolutions of the voltage scale model (superindex "v") compared with the original model under chosen input-current profile.

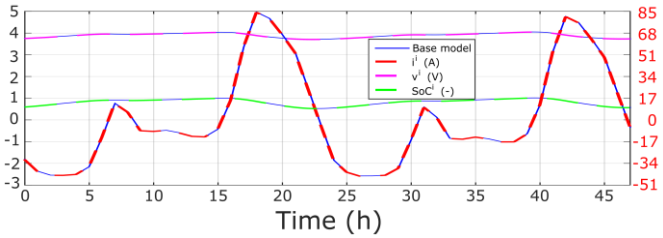

Fig. 2c. Voltage, current (right red axis scale) and SoC evolutions of the current scale model (superindex "i") compared with the original model under chosen input-current profile.

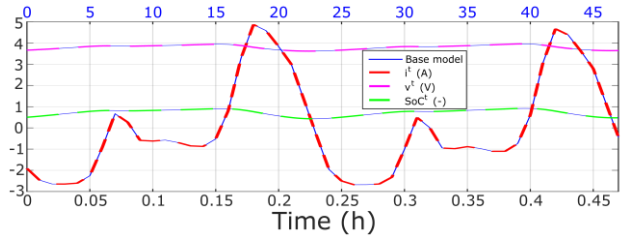

Fig. 2d. Voltage, current and SoC evolutions of the time scale model (lower black axis scale) (superindex "t") compared with the original model (upper blue axis scale) under chosen input-current profile.

A battery system is composed of an array of parallel and/or series connected battery cells. It can be demonstrated that a defined ratio between the parameter sets of both models exists. **Voltage scaling**. For batteries in series connection $v_{eq}(t)=n_s v(t)$ and $i_{eq}(t)=i(t)$ do hold. Additionaly $Q_{eq}=Q$ implying $SoC_{eq}(t)=SoC(t)$. From these variables equalities follow that a series connection is equivalent to voltage scaling the original model by a factor $k_v=n_s$.

Current scaling. Similarly as in the case of voltage scaling, it can be easily shown that the case of current scaling with a relation $k_i=n_p$ is equivalent to a parallel connection of n_p batteries.

Time scaling. None of the previous connections (neither series nor parallel) yields a time scaling procedure. This can be easily seen in the fact that the current filter time constant, T_f, that inherently represents electrochemical dynamics, will not be affected. This introduces the problems in physical emulation discussed ahead in § IV-D.3.

A. Design of experiments

In order to test the scaling procedure four configurations have been implemented. While the first three configurations are used to validate voltage- and current-scaling procedure, the last configuration serves to test the time-scaling procedure and exhibits the physical emulation problem in time contraction.

- **Configuration I:** 1 branch of 6 batteries in series (1x6 configuration→ $k_v = 6 \wedge k_i = 1$)
- **Configuration II:** 2 branches of 3 batteries in series (2x3 configuration→ $k_v = 3 \wedge k_i = 2$)
- **Configuration III:** 3 branches of 2 batteries in series (3x2 configuration→ $k_v = 2 \wedge k_i = 3$)
- **Configuration IV:** 5 batteries in parallel (5x1 configuration→ $k_v = 1 \wedge k_i = 5$)

These configurations have been determined by the available number of batteries and current probes, as well as by the current limitation of the controllable power sources used in the experimental set-up described next.

B. Test bench

In order to test a battery (or battery array up to 6 Lithium Ion (LiFePo4) batteries - Mottcell 3.2V 39Ah) a remote controllable bidirectional source of voltage/current (configured by a Power source PSI 9080-510 and a Controlled Load ELR 9080-510) is used with configurable charge and discharge profiles (achieved using a dSPACE system). Over- and under-voltage protections, as well as thermal protection are implemented. To obtain more accurate and faster sampling rate a SEFRAM Data acquisition System with 3 Clamps on probe HIOKI 3274 is used. This test bench allows for voltage and current control of user defined profiles, and measurements of each battery voltage, up to 3 currents and several temperatures (environment, terminals, body, etc.).

C. Current profiles tested

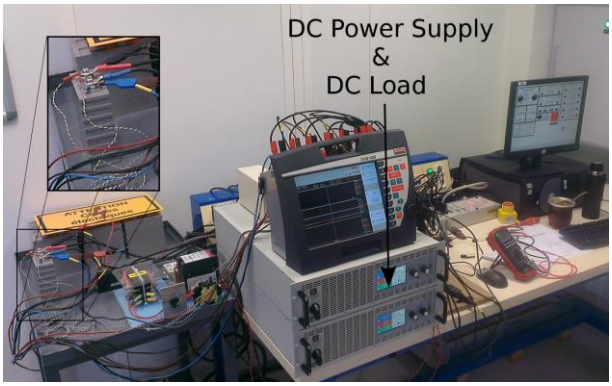

Fig. 3. Battery test bench developed at LAPLACE Laboratory.

The battery systems were tested under two different current profiles: the HPPC profile and the FTP profile. The **HPPC profile** was designed in order to measure the dynamic power capability over a device's usable charge and voltage range [19],[20]. It consists in a series of discharge and charge pulses of constant current at different SoC, see Fig. 4. Pulse duration and intensity depend on test objectives and, as suggested in [17] it is used to identify model parameters.

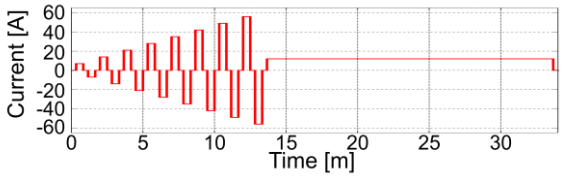

Fig. 4. Extract of the HPPC profile: a cyclic charge/discharge process followed by SoC variation.

The **FTP profile** is a realistic current profile for battery-powered electric vehicles subject to the commonly used FTP-75 driving cycle. It was extracted from [21] and adapted for the battery configuration under study, see Fig. 5.

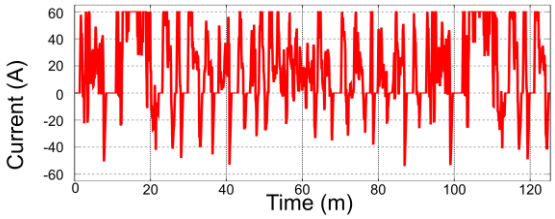

Fig. 5. Current profile demanded to the battery system of a battery-powered electric vehicle to complete FTP-75 speed profile.

Complementary to the HPPC profile, the FTP profile has been selected for validation of the scaled models due to its rich dynamic contents, as it reflects the diversity of solicitations to batteries embedded in EV, HEV and PHEV [22]. It seems also relevant in terms of frequency dynamics for other fields of applications.

D. Validation of the physical scale model

1) Base Model Identification

The scaling procedure was applied to a battery cell whose model is considered as the original system. Its parameters have been estimated averaging six sets of data obtained running the HPPC profile on six batteries of the same type and identifying each parameter set following a method given in [17]. Each parameter of this base average model –to be scaled in voltage, current and time– is the mean value of the corresponding parameters of the six sets. In this way the effect of the battery dispersion is reduced. The resulting set is given in Table IV.

TABLE IV
PARAMETER SET OF BASE AVERAGE MODEL FOR ONE BATTERY CELL.

Parameter	Q (Ah)	E_0 (V)	K_1 (mV/Ah)	A (mV)	B (Ah^{-1})	R $(m\Omega)$	K_2 $(m\Omega)$	Tf (s)
X_base	36.82	3.259	0.240	74.50	0.033	6.362	0.747	88.33

2) Voltage- and current-scaling

According to the scaling method, starting from the base model parameters, the equivalent models for the battery systems for Configuration I, II and III were calculated. Afterwards, each physical realization was tested under the HPPC profile and parameters were identified and compared with the previously calculated parameters, see Table V. Even though a notorious discrepancy exists among some of the parameters (up to 628% for the worst case), the dynamic evolution of the variables are not appreciably affected. This is due to the fact that the battery voltage sensitivity associated to those parameters is low[1].

[1] See Sensitivity Analysis in Appendix A.

TABLE V
PARAMETER VALUES CALCULATED (CAL) BY SCALING METHOD, ESTIMATED (EST) BY PHYSICAL BATTERY TESTING, AND THE RELATIVE ERROR (ERR) BETWEEN THEM FOR CONFIGURATION I, II AND III.

Parameter	$Q\ (Ah)$	$E_0\ (V)$	$K_1\ (mV/Ah)$	$A\ (mV)$	$B\ (Ah^{-1})$	$R\ (m\Omega)$	$K_2\ (m\Omega)$	$Tf\ (s)$
X_C-I_cal	36.82	19.553	1.438	446.97	0.033	38.172	4.481	88.33
X_C-I_est	36.79	19.593	1.427	405.89	0.032	38.184	4.429	87.94
X_C-I_err	-0.08%	0.20%	-0.82%	-9.19%	-4.04%	0.03%	-1.14%	-0.44%
X_C-II_cal	73.64	9.776	0.360	223.49	0.017	9.543	1.120	88.33
X_C-II_est	72.80	9.756	0.321	269.12	0.015	9.346	1.040	71.06
X_C-II_err	-1.14%	-0.21%	-10.80%	20.42%	-9.42%	-2>06%	-7.17%	-19.55%
X_C-III_cal	110.45	6.518	0.160	148.99	0.011	4.241	0.498	88.33
X_C-III_est	112.36	6.616	0.222	115.92	0.081	4.535	0.573	68.10
X_C-III_err	1.73%	1.51%	39.00%	-22.20%	628.06%	6.93%	15.05%	-22.90%

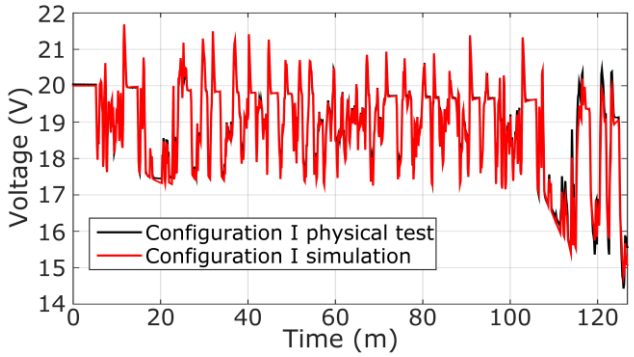

Fig. 6. Voltage response in Configuration I under FTP current profile.

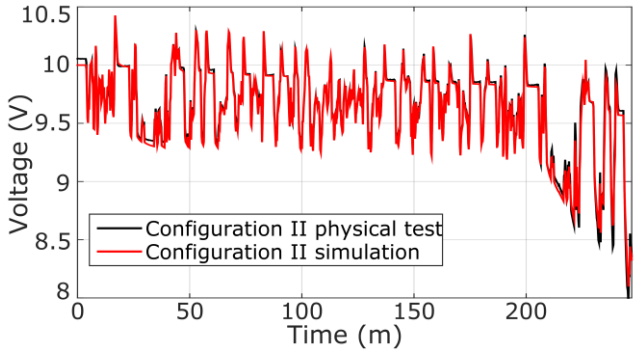

Fig. 7. Voltage response in Configuration II under FTP current profile.

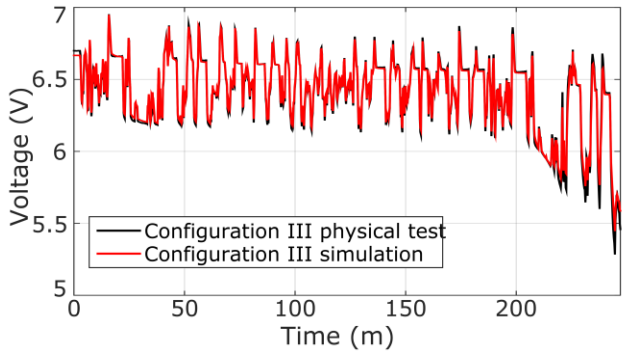

Fig. 8. Voltage response in Configuration III under FTP profile.

This can be corroborated comparing the results of the physical tests and the scale models simulations under the FTP profile, Figs. 6, 7 and 8.

Fig. 6 shows the voltage response under the FTP current profile of Fig. 5. It can be seen that the calculated scaled model reproduces the voltage dynamics for the complete test. The Root Mean Square Error (RMSE) is 56mV and the Maximal Absolute Error (MAE) is 1V ($\sim 5\% E_0$).

Similar calculations were done after testing Configuration II and III –with results shown in Figs. 7 and 8– giving RMSE of 20.31mV and 19.71mV, respectively, and MAE of 208mV and 176mV, respectively.

These results validate the statement of equivalence between series and parallel connection with voltage and current scaling procedure and, as a consequence, the achievement of *dimensional similarity* among the three configurations.

3) Time-scaling

The focus in this scaling process is to accelerate the physical emulation of the batteries, i.e., to reduce the testing time. For this purpose Configuration IV (5 batteries connected in parallel) is considered as the original system (instead of a single battery to be scaled, as done in the other configurations). In order to reduce the test time by a factor of 5, the parameters are scaled (see Table I) with $k_i = 1$, $k_v = 1$ and $k_t = 5$. In this case, there is no possible battery combination (series or parallel connections) yielding a model with the same parameter values than the calculated by the time-scaling method. The closest physical realization of this parameterization using the given batteries is a single battery, see Table VI.

The validation tests consisted in two physical tests and a simulation run. In the first test a 10 hours length FTP profile was used for Configuration IV (blue curve on Fig. 9) while a compressed 2 hours length FTP profile (accelerated profile) was used for both single battery physical model test (black curve on Fig. 9) and the simulation test of the scaled mathematical model corresponding to Configuration IV (red curve on Fig. 9). The voltage outputs of these three tests are mathematical model corresponding to Configuration IV (red curve on Fig. 9). The voltage outputs of these three tests are shown in Fig. 9. A simple axis compression of the 10hours test is shown on the blue curve for comparison with the accelerated ones. It can be seen that the mathematical scale model fits much better the original, uncompressed, system than the closest physical realization

The validation tests consisted in two physical tests and a simulation run. In the first test a 10 hours length FTP profile was used for Configuration IV (blue curve on Fig. 9) while a compressed 2 hours length FTP profile (accelerated profile) was used for both single battery physical model test (black curve on Fig. 9) and the simulation test of the scaled mathematical model corresponding to Configuration IV (red

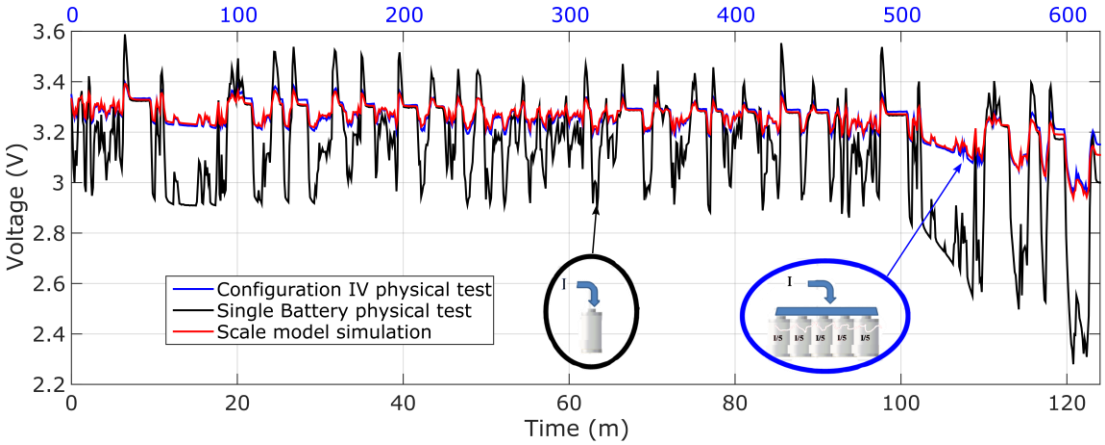

Fig. 9. Battery voltage evolution under FTP current profile of Configuration IV (blue time axis), single battery , and exact time-scaled model simulation.

curve on Fig. 9). The voltage outputs of these three tests are shown in Fig. 9. A simple axis compression of the 10hours test is shown on the blue curve for comparison with the accelerated ones. It can be seen that the mathematical scale model fits much better the original, uncompressed, system than the closest physical realization.

Comparing the voltage response of both physical tests an important difference is noticed. The RMSE is 195.47mV (~6%E_0) and MAE is 702.8mV (~22%E_0). This voltage error is mainly due to the fact that the battery resistances are 5 times bigger than desired and the voltage sensitivity to those parameters is considerable.

On the other hand, the comparison between the tests on the original Configuration IV and the mathematical scale model shows that the RMSE is reduced to 12.48mV (~0.4% E_0) and the MAE to 60.3mV (~2% E_0).

TABLE VI.
SET OF PARAMETER VALUES OF CONFIGURATION IV (BLUE CURVE), SINGLE BATTERY MODEL (BLACK CURVE) AND TIME-SCALED MODEL (RED CURVE).

Parameter	Q (Ah)	E_0 (V)	K_1 (mV/Ah)	A (mV)	B (Ah^{-1})	R $(m\Omega)$	K_2 $(m\Omega)$	Tf (s)
X_C-IV 2	184.09	3.259	0.048	74.50	0.007	1.272	0.149	88.33
X_C-IV_sca	36.82	3.259	0.240	74.50	0.033	1.272	0.149	17.67
X_Single-Bat	36.82	3.259	0.240	74.50	0.033	6.362	0.747	88.33

V. CONCLUSIONS

This article applied the concept of dimensional similarity to a battery model in order to scale a battery system in size and time. Even though this battery model is nonlinear, a re-parameterization is possible in order to achieve a perfect voltage-, current- and time-scaling in the mathematical scale model. Even if not as flexible as mathematical scale models, physical scale models are most interesting and useful because they allow to study also the influence of unmodeled physics such as the influence of temperature, auto-discharge and/or ageing effects in this application case. In the case of voltage- and current-scaling the physical scale model could be implemented using series and parallel connections of the same base battery. This is useful to conduct experiments with reduced power size of a battery bank. It is worth mentioning that physical scaling is limited to an integer-number scaling of the base battery.

In the particular case of time-scaling, a perfect physical implementation is not possible using the same base battery of the original system. This is due to the physical constraints imposed on the parameters of a given battery. This problem certainly hinders the physical emulation in compressed time of just a battery or battery pack, but is not an obstacle for the emulation of a system involving batteries. Indeed, as the mathematical scale model can always be achieved for the three scaling methods without restrictions in the scale factors, it can be implemented and run in real time on a computer device embedded in a physical set up completed with the physical emulator of the rest of the system under study, i.e., a HIL-approach solves the problem. This mixed physical-numerical approach allows designers to emulate any kind of electric networks involving generation, storage and/or load devices and to take benefit of time contraction effects to realize tests with reduced virtual time scale. This reveals that the usefulness for simulation of this method lies mainly in the rea l-time implementation of the numerical emulators as part of the HIL-system. As wind turbines and photovoltaic panels (as well as any other component of a power system) can be scaled with this technique (an issue being subject of ongoing research), their numerical scale models could also be integrated in a HIL-system for the experimental study on a test-bench, for instance, of the behavior of a smart grid being part of a distributed generation system.

APPENDIX

A. SENSITIVITY ANALYSIS

TABLE A
SENSITIVITY COEFFICIENT OF BATTERY VOLTAGE FUNCTION

SoC	φ_Q	φ_{E_0}	φ_{K_1}	φ_A	φ_B	φ_R	φ_{K_2}
1.05	0.002	0.976	0.000	0.024	0.001	0.070	0.165
0.85	-0.004	0.982	0.000	0.019	-0.003	0.071	0.033
0.65	-0.008	0.987	0.001	0.015	-0.006	0.071	0.019
0.45	-0.011	0.992	0.003	0.012	-0.008	0.071	0.019

[2] Set of parameters of Configuration IV calculated using the base battery model parameterization and the current scaling procedure (ki=5) validated

0.25	-0.016	0.999	0.008	0.009	-0.008	0.072	0.034
0.05	-0.063	1.046	0.054	0.007	-0.009	0.075	0.177

Given a function, v, the sensitivity coefficient φ_{X_i} for a particular parameter X_i can be calculated as

$$\varphi_i = \frac{\partial v}{\partial X_i}\frac{X_i}{v}\Big|_{v=v_k}$$

where the quotient, X_i/v, normalizes the coefficient.

Table A resumes the calculations of the voltage sensitivity for the parameters in five different SoC and considering $i = i^* = i_{nom}$.

ACKNOWLEDGMENTS

The authors thank CONICET (the Argentine National Council for Scientific and Technological Research), SeCyT-UNR (the Secretary for Science and Technology - UNR), ANPCyT (PICT 2012 Nr. 2471) and the scholarship program Saint-Exupéry for their financial support, as well as the Facultad de Ciencias Exactas Ingeniería y Agrimensura for providing workplace. Authors also thank Ing. Daniel Alba for fruitful discussions related to battery modeling and testing.

REFERENCES

[1] P.C. Krause, O. Wasynczuk, and S. D. Sudhoff, "Analysis of Electric Machinery and Drive Systems", 2nd ed. New York: IEEE Press, 2002.

[2] W. Leonhard, "Control of Electric Drives", 3rd ed., Berlin New York: Springer, 2001.

[3] P.W. Bridgman, "Dimensional Analysis", 2nd ed., Yale University Press, 1931.

[4] T. Szirtes, "Applied Dimensional Analysis and Modeling", 2nd ed., Butterworth-Heinemann, 2006.

[5] B. Kittirungsi, H.K. Fathy, and J.L. Stein, "An efficient scaling methodology for dynamic models using dimensional and activity analyses", in *ASME 2006 International Mechanical Engineering Congress and Exposition* (IMECE2006-14587), Chicago, 2006.

[6] C. Seitl, J. Kathan, G. Lauss, and F. Lehfuss, "Power hardware-in-the-loop implementation and verification of a real time capable battery model", in *Industrial Electronics (ISIE)*, 2014 IEEE 23rd International Symposium on , vol., no., pp. 2285-2290, 1-4 June 2014.

[7] N. Shidore, N. Kim, R. Vijayagopal, D. Lee, A. Rousseau, J. Kwon, B. Honel, and E. Haggard, "Battery in the loop: Battery evaluation in a systems context," in *Transportation Electrification Conference and Expo (ITEC), 2014 IEEE* , vol., no., pp.1-9, 15-18 June 2014..

[8] M. Lemaire, P. Sicard, and J. Belanger "Prototyping and Testing Power Electronics Systems Using Controller Hardware-In-the-Loop (HIL) and Power Hardware-In-the-Loop (PHIL) Simulations," in *Vehicle Power and Propulsion Conf. (VPPC) IEEE* , pp.1-6, 19-22 Oct. 2015.

[9] J. V Barreras; M Swierczynski, E. Schaltz, S. J. Andreasen, C. Fleischer, D. Uwe Sauer, and A.E.Christensen, "Functional analysis of Battery Management Systems using multi-cell HIL simulator," in *Ecological Vehicles and Renewable Energies (EVER), 2015 Tenth International Conf. on* , vol., no., pp.1-10, March 31 - April 2 2015.

[10] M. D. Petersheim, and S.N.Brennan, "Scaling of hybrid electric vehicle powertrain components for hardware-in-the-loop simulation," in *Control Applications, 2008. CCA 2008. IEEE International Conference on* , vol., no., pp.720-726, 3-5 Sept. 2008.

[11] R.S. Razavian, A. Taghavipour, N. L.Azad, and J. McPhee, "A battery hardware-in-the-loop setup for concurrent design and evaluation of real-time optimal HEV power management controllers", International Journal of Electric and Hybrid Vehicles. 5, 3, 177-194, 2013.

[12] E. Buckingham, "On physically similar systems: illustrations of the use of dimensional equations", Phys Rev 1914; 4(2):345-76.

[13] P. Du, and N. Lu, 2015. *Energy Storage for Smart Grids*, Boston, Academic Press.

[14] S. F. Tie, and C. W. Tan, "A review of energy sources and energy management system in electric vehicles," Renewable and Sustainable Energy Reviews, vol. 20, pp. 82–102, 2013.

[15] C. Dumbs, "Développement d'outils pour l'analyse des systèmes hybrides photovoltaïque-diesel," Ph.D. dissertation, Centre d'Energétique, Ecole des mines Paris, 1999.

[16] O. Tremblay, and L. A. Dessaint, "Experimental validation of a battery dynamic model for EV applications", *World Electric Vehicle Journal. Vol. 3*, no. 1, pp. 1–10, 2009.

[17] J. M. Cabello, E. Bru, X. Roboam, F. Lacressonniere, and S. Junco. "Battery dynamic model improvement with parameters estimation and experimental validation", IMAACA 2015, Bergeggi, Italy.

[18] R. Rigo-Mariani, "Méthodes de conception intégrée dimensionnement-gestion par optimization d'un microréseau avec stockage," Ph.D. thesis, GEET, LAPLACE, INP Toulouse, France, 2014.

[19] G. Hunt, *PNGV battery test manual*. INEEL,, Rev. 3, 2001.

[20] J. Shim, and K. A. Striebel, "Characterization of high-power lithium-ion cells during constant current cycling: Part I. Cycle performance and electrochemical diagnostics". *Journal of Power Sources. Vol. 122*, pp 188–194, 2003.

[21] M. Carignano, J. M. Cabello, and S. Junco, "Sizing and performance analysis of battery pack in electric vehicles". *Biennial Congress of Argentina (ARGENCON) IEEE*. pp. 240-244, 2014.

[22] K. Fleurbaey, N. Omar, M. El Baghdadi, J. M. Timmermans and J Van Mierlo, "Analysis of Hybrid Rechargeable energy Storage Systems in Series Plug-In Hybrid Electric Vehicles Based on Simulations". *Energy and Power*, 6, pp. 195-211, 2014.

Javier M. Cabello received the Electronic Engineering degree from the Facultad de Ciencias Exactas Ingeniería y Agrimensura of Universidad Nacional de Rosario, Rosario, Argentina, in 2012. He is currently pursuing the Ph.D. degree in engineering at Universidad Nacional de Rosario. His research interests include optimal sizing of components and energy management strategies in Smart Grids applications.

Xavier Roboam received the Ph.D. Degree of Université de Toulouse, France in 1991. He is full-time researcher (Directeur de Recherches CNRS) in the Laboratory of Plasma and Conversion of electrical Energy (LAPLACE) of Toulouse since 1992 where he develops design methodologies specifically oriented towards multi-fields devices for embedded or renewable energy systems.

Sergio Junco received the Electrical Engineer degree from the Universidad Nacional de Rosario in 1976. Since 1982 he is a member of this University's faculty, currently a Full-time Professor of System Dynamics and Control and Head of the Automation and Control Systems Laboratory. His current research interests are in modeling, simulation, control and diagnosis of dynamic systems, with applications to electrical drives, power electronics, mechatronics and smart grids. He has developed, and currently teaches, several courses on System Dynamics, Bond Graph Modeling and Simulation.

Eric Bru received the MSc electric engineering degree from l'École d'ingénieurs du CNAM, Toulouse, France, in 2005. He joined the LAPLACE as test engineer in 2006.

He develops test benches devoted to HVDC networks, renewable energy systems, hybridization devices with electrical storage such as ultracapacitor or electrochemical accumulators in the GENESYS-Team.

Fabien Lacressonniere received the Ph.D degree in Electrical Engineering from the Université d'Artois, Béthune, France, in 2005.

He is currently an Associate Professor at the Université Paul Sabatier de Toulouse – IUT de Tarbes where he teaches on electric actuators and power electronics. His research activity takes place in Laboratoire Plasma et Convertion d'Energie, Toulouse. His major research interest is on the modeling of electrochemical accumulators, and more particularly of Li-ion batteries.